Integrating structural, hydraulic and geochemical evidence: A step towards understanding fluid flow through clay-rich formations

Martin Mazurek

Rock/Water Interaction Group (GGWW), Institutes of Geology and of Mineralogy and Petrology, Baltzerstr. 1, University of Bern, CH-3012 Bern, Switzerland

Argillaceous rock formations are targets of exploration for radioactive waste disposal sites in several countries. Groundwater flow in most indurated argillaceous rocks is very limited and occurs (if at all) mainly in brittle discontinuities, such as faults. On the basis of surface observations, core logging and hydraulic measurements in boreholes penetrating an argillaceous marl formation in the Swiss Alps (Figure 1), the relationships between internal fault architecture, larger-scale arrangement of the fault network and fault transmissivity are explored. Only a fraction of all faults observed in the cores correlates with water inflow points into the boreholes, and this is taken as evidence of variable transmissivity within each fault. Such flow channeling is also supported by geologic evidence (Figure 2).

Stochastic discrete fracture network models are used for the upscaling of measured fault transmissivities, namely for the calculation of effective hydraulic conductivities (K_{eff}) of model cubes with lengths of side of 50-500 m. Input data to these models include size, spacing, orientation, heterogeneity (flow channeling) and transmissivity of the faults. Fault size is not well known, but a sensitivity analysis shows that even the extreme assumption of infinite size yields K_{eff} only less than 1 order of magnitude higher when compared to the base case (Table 1). The effect of different arrangements of flow channels within each fault is also explored but has no appreciable effect on K_{eff}. It is concluded that calculated values for K_{eff} are robust because those input parameters that are least adequately known have only limited effects on the model results.

center of model cube, m below surface	log (K_{eff}, m/s) for fault size = 20 x fault thickness	log (K_{eff}, m/s) for fault size = 100 x fault thickness	log (K_{eff}, m/s) for fault size = 200 x fault thickness	log (K_{eff}, m/s) for fault size = infinity
190	-9.5	-8.4	-8.5	-7.5
290	-9.9	-8.5	-8.7	-7.8
390	-10.3	-9.5	-9.7	-9.4
490	-12.0	-11.3	-11.4	-10.9
590	*	-12.9	-12.9	-12.5
690	*	-13.0	-12.9	-12.1

Table 1: Sensitivity analysis of fault size in discrete fracture-network realizations. Calculated log (K_{eff}) are averages of several realizations. *: Ca. 90% of all network realizations yield unconnected networks (i.e. no fracture flow), ca. 10% yield K_{eff} below 10^{-13} m/s, which is the estimated hydraulic conductivity of the rock volume between water-conducting features

Fluid chemistry was studied by a number of techniques. Fluid inclusions record the conditions of maximum burial and regional low-temperature metamorphism, whereas fluid samples and hydraulic tests derived from deep boreholes reflect present-day, near-surface conditions. The characterization of the different types of fluids (Figure 3) places constraints on the geochemical and hydraulic evolution of low-permeability argillaceous rocks during uplift and exhumation.

Fluid inclusions were studied by microthermometry and sampled directly by decrepitation techniques. They contain a two-phase system consisting of an aqueous fluid and a coexisting methane-rich gas (T = 190 - 250 °C, $P_{lith} \approx 2500$ bar). Bulk and isotopic compositions of aqueous fluid inclusions are consistent with a mixture of connate seawater and water derived from the dehydration of clay minerals. Methane was generated *in situ* by thermal cracking of kerogen. Textural evidence and stable isotopic signatures of carbonates in veins and in the rock matrix indicate local buffering of fluid compositions and very low water/rock ratios. Free fluids residing in the present-day fracture and matrix porosity consist of methane-saturated Na-Cl groundwater with minute amounts of free methane gas which occurs in druses. Their chemical and isotopic compositions are very similar to those of the fluid inclusions, suggesting a common origin. Post-metamorphic admixtures of externally derived waters cannot be identified, and it is suggested that present-day Na-Cl groundwaters that occur in the central parts of the marl have resided in the formation since the time of metamorphism some 20 Ma b.p. The only major change in the fluid composition has been the outgassing of methane from the formation, most probably by diffusion.

The hydraulic regime during metamorphism was characterized by localized fluid underpressures in open veins because widely scattered, sub-hydrostatic pressures were often identified in fluid inclusions. The central part of the argillaceous rock body, approximately coinciding with the region where Na-Cl groundwaters occur, has sub-hydrostatic pressures today, as indicated by hydraulic tests in deep boreholes. Remarkably, this zone yields very low K_{eff} on the basis of fracture network modelling, and, under certain assumptions, the model yields unconnected networks (Table 1).

Both the closed-system behaviour derived from the chemical and isotopic characteristics of the fluids and the (recurrent or continuous) existence of hydraulic underpressures suggest very low permeabilities of argillaceous rocks during metamorphism and throughout subsequent uplift and exhumation. All fluids present in the central parts of the formation are either connate or produced *in situ.* Even though major events of brittle faulting and unloading due to uplift occurred since the peak of metamorphism, fluid flow through the formation has been negligible.

References

Mazurek, M., Lanyon, G.W., Vomvoris, S. and Gautschi, A. 1999: Derivation and application of a geologic dataset for flow modelling by discrete fracture networks in low-permeability argillaceous rocks. Journal of Contaminant Hydrology 35, 1-17

Mazurek, M. 1999: Evolution of gas and aqueous fluid in low-permeability shales during uplift and exhumation of the central Swiss Alps. Applied Geochemistry 15, 223-246

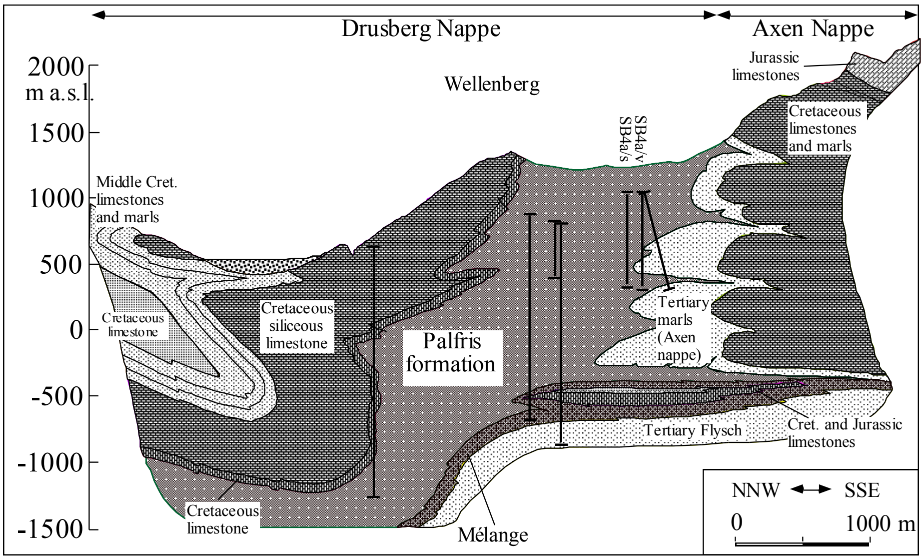

Figure 1: Geological profile through the Wellenberg area. Positions of boreholes (thick lines) are projected into the plane of the profile.

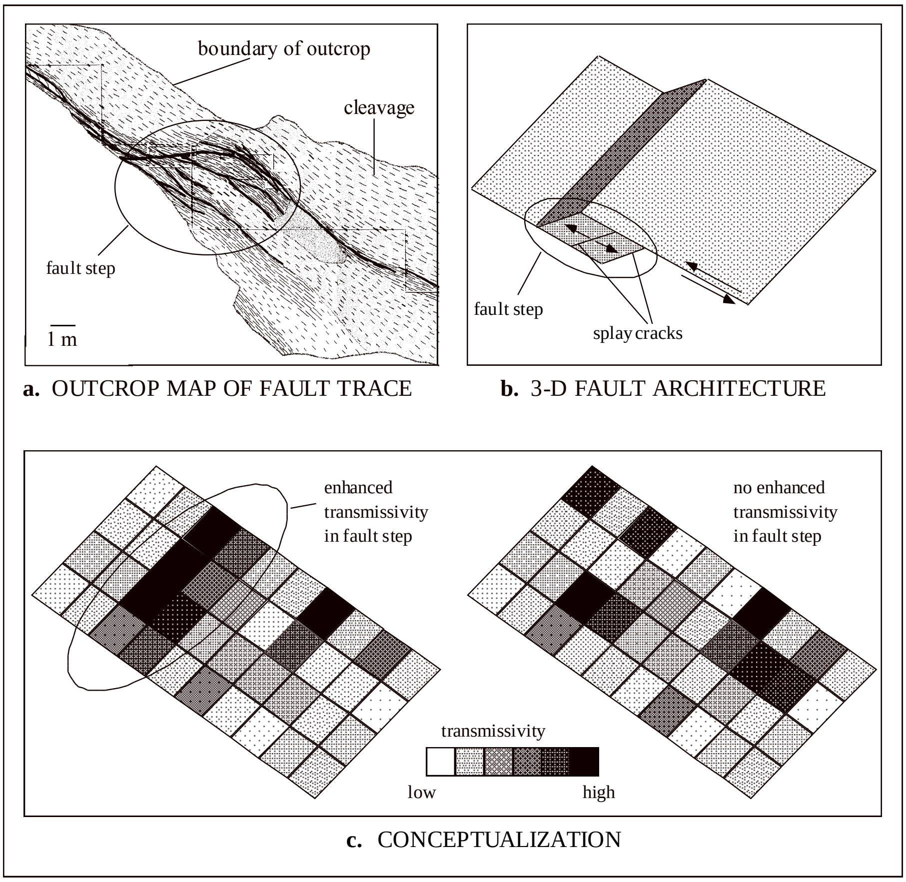

Figure 2: Anatomy, mechanistic interpretation and conceptualization of a fault cross cutting the Palfris formation.

a. Map of a surface outcrop
b. 3-dimensional sketch view of the fault from a., with mechanistic interpretation of the deformation mechanism
c. Two alternative conceptualizations of the internal fault structure for use in fracture network models.

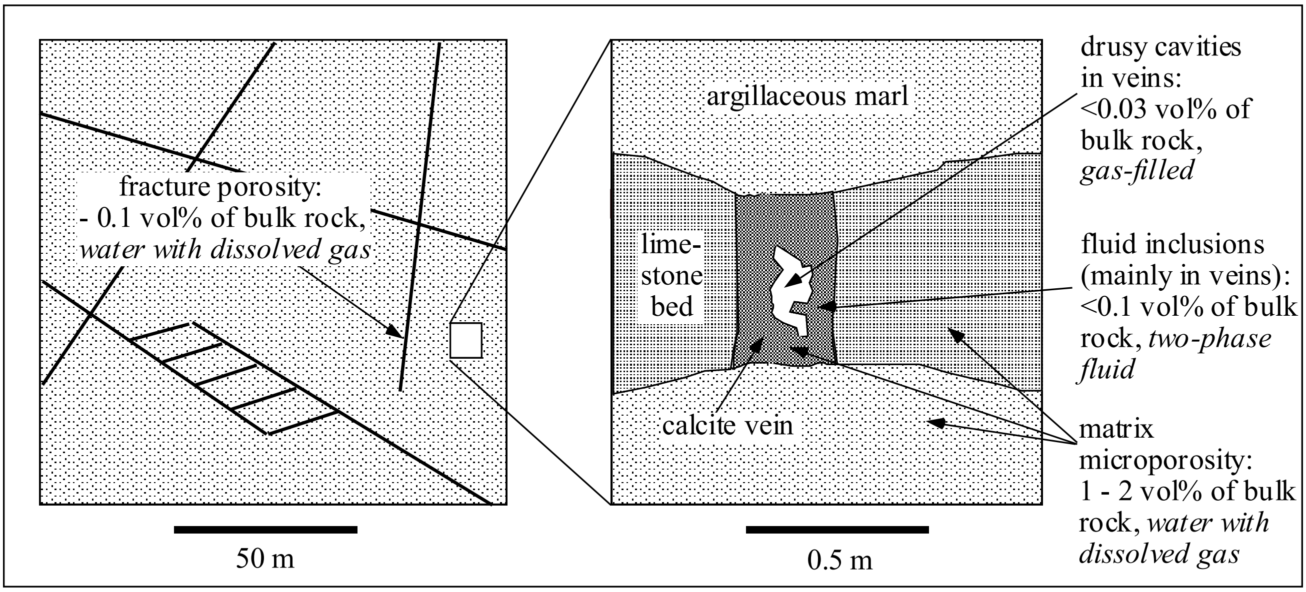

Figure 3: Types of porosities and fluid domains.